

Mathematical Modeling for the Pultrusion of Polymethyl Methacrylate Based Composites

Chin-Hsing Chen

Department of Chemical and Materials Engineering, Chinese Culture University, Yang-Ming-Shan, Taipei, Taiwan

Received 22 February 2011; accepted 24 April 2011

DOI 10.1002/app.34740

Published online 23 August 2011 in Wiley Online Library (wileyonlinelibrary.com).

ABSTRACT: The thermokinetic behavior of polymethyl methacrylate (PMMA)-based composites during the pultrusion of glass fiber reinforced composites was investigated using a mathematical model accounting for the heat transfer and heat generation during the reaction. The equations of continuity and energy balance, coupled with a kinetic expression for the reaction system were solved using a finite difference method to calculate the temperature profiles in the thickness direction in a rectangular pultrusion die. A kinetic model, $\frac{dP}{dt} = -\eta A_o \exp\left(-\frac{E_p}{RT}\right) (2[I]_o - [Z]_o) P^m \left(1 - \frac{P}{P_r}\right)^n (1 - \exp(-k_d(t - t_z)))$, was proposed to describe the reaction behavior of a PMMA resin. Kinetic parameters for the model were found from isothermal differential scanning calorimetry (DSC) scans using a multiple regression tech-

nique. The kinetic parameters $\eta A_o = 1.459 \times 10^9 \text{ min}^{-1}$, $E_p = 10.62 \text{ kcal/mol}$, $m = 1.095$, and $n = 0.893$ were obtained. The predictions of the model will be compared with experimental results. It can be found that the theoretical predicted values of temperature profiles along the pultrusion die length were in good agreement with experimental data, which implies that the mathematical model was suitable for the pultrusion processes. © 2011 Wiley Periodicals, Inc. *J Appl Polym Sci* 123: 2228–2233, 2012

Key words: pultrusion; polymethyl methacrylate; fibers; differential scanning calorimetry; kinetic; mathematical model; composites

INTRODUCTION

Pultrusion was an efficient manufacturing processes for fabricating polymer composite parts of constant cross-section.^{1,2} Pultruded composites showed the properties such as high toughness, corrosion resistance, high strength-to-weight ratio, excellent electrical insulation, abrasion resistance, and dimensional stability, which have been widely used in corrosion resistant parts, electronic and electrical materials, sporting goods, construction, transportation, chemical engineering, aircraft and aerospace, and so on.^{3,4} The pultruder consisted of a fiber roving shelf, fiber guides, fiber drying chamber, resin wet-out tank, heated matched metal die, synchronized pullers, and cut-off saw.⁵ Figure 1 showed a schematic representation of *in-situ* pultrusion process.⁶ This technology offered the advantages of continuous production, integration of fiber impregnation and composite consolidation in the same process. This simplicity, efficiency, and flexibility of this process make it one of the most interesting methods for the fabrication of continuous fiber composite products with constant cross-section.⁷ Most of the literature published^{8–13}

discussed its applications, some aspects of pultruded composites and the pultrusion process from the point view of monitoring the quality of incoming resins. There is several work^{14–16} had been said about the fundamental aspects of this process. The process was difficult to control unless one knows how to handle the exothermic chemical curing reactions which took place inside a pultrusion die.

Recently, a variety of experimental techniques had been developed to study the curing reaction of resins. Among them, the technique of isothermal differential scanning calorimetry (DSC) had been found to provide a convenient and useful method to monitor the course exothermic curing reactions.^{1,2,17} The method was based on the measurement of the rate at which heat was generated in an exothermic chemical reaction. With the assumption that the heat generated by the chemical reaction was proportional to the extent of reaction, the kinetic parameters can be obtained from simulation.

To manufacture pultruded composites with consistent quality, it was essential to develop a strategy for controlling the pultrusion process on the basis of fundamental investigation. To achieve a uniform degree of curing in the pultruded composites. The temperature profile in the pultrusion die was the most important condition. The temperature model predicts the temperature of the pultruded composites as a function of distance from the composite

Correspondence to: C.-H. Chen (cjx@faculty.pccu.edu.tw).

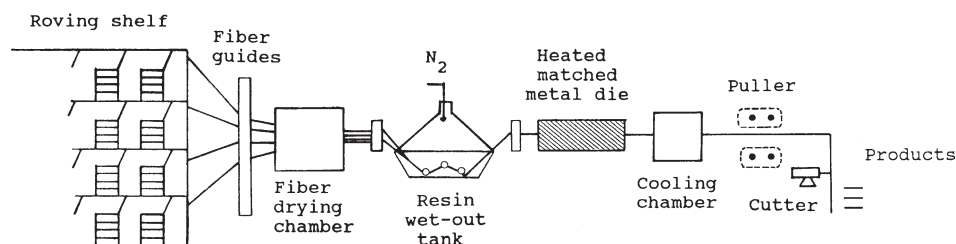


Figure 1 A schematic representation of *in situ* pultrusion process.

centerline and location in the pultrusion die. The composite was treated as a transversely isotropic, long slab of constant height with either prescribed boundary temperature or prescribed heat flux from the surfaces. Hence, heat transfer was considered through the thickness only, and issues of axial heat transfer, viscous dissipation.¹⁸ It should be pointed out that control of the temperature profiles in the thin direction in a rectangular pultrusion die and radial direction in a cylindrical pultrusion die was very important. It was therefore important to develop a mathematical model for simulating the pultrusion process and ultimately for controlling the process.^{1,19–21}

The original aspect of this study was to develop a mathematical model including the equations of continuity and energy balance, coupled with a kinetic model for the reaction system are solved using a finite difference method to calculate the temperature profiles in the thickness direction in a rectangular pultrusion die, and the kinetic model are set up by myself. By introducing a kinetic model using isothermal DSC scanning and heat transfer, which were relevant for the pultrusion of polymethyl methacrylate (PMMA) resin. The predictions of the model will be compared with experimental results.

EXPERIMENTAL

Materials

The methyl methacrylate (MMA) monomer used in this research was a purified industry grade and was supplied by the Kaohsiung Monomer Co., Taiwan. The PMMA prepolymer was synthesized in this study. The initiator benzoyl peroxide (BPO) used was a guaranteed reagent, which was obtained from the Kanto Chemical Co., Japan. The continuous E-glass fiber roving reinforcement used was 764-NT-218 and supplied by PPG Co., which had a filament diameter of 13.1 μm , a tensile strength of 206 ksi, and a density of 2.54 g cm^{-3} .

Procedures

The PMMA prepolymer was blended in 100/0.5 weight ratios of MMA monomer/BPO in a water

bath at 55°C. The reaction was permitted to exothermic upon stirring and under a nitrogen blanket until a suitable prepolymer viscosity was reached.

DSC was used to investigate the reaction behavior of PMMA prepolymer. A 5–10 mg PMMA prepolymer was placed in the DSC cell. The aluminum sample pan was tightly sealed and an isothermal DSC runs were made at 80, 85, 90, 95, and 100°C. Following an isothermal runs, the sample was further heated to 150°C at a heating rate of 10°C/min.

To accurately determine the degree of reaction, Fourier infrared (FTIR) spectroscopy was used to determine the number of C=C double bonds in a PMMA resin system before polymerization began and the amount of residual double bonds after the sample was reacted (i.e., after the completion of isothermal reaction followed by the heating of the sample to 150°C). This information together with the information on the heat generated in the isothermal runs was used to determine the rate of polymerization, as well as the degree of polymerization during the entire period of the isothermal reaction.

Apparatus and measurement

The pultrusion machine was custom-designed. It consisted of multiple heating zones and a pultrusion die with dimensions of 82 × 1.27 × 0.319 cm (length × width × thickness). The surfaces of the stainless steel die were treated by chrome plating. The calorimetric measurements were conducted using a DuPont 2000 differential scanning calorimeter with nitrogen as the flushing gas. The temperature and power calibration of the DSC were optimized within the temperature range of 30–300°C using indium as the DSC calibration standard. FTIR measurements were carried out with a Model FTIR-5300 (Jasco Co., Japan).

RESULTS AND DISCUSSION

Kinetic analysis

To determine the degree of reaction when the PMMA was polymerized, it can be discussed by using FTIR spectra. Figure 2 showed the FTIR spectra of the PMMA resin before and after reaction.

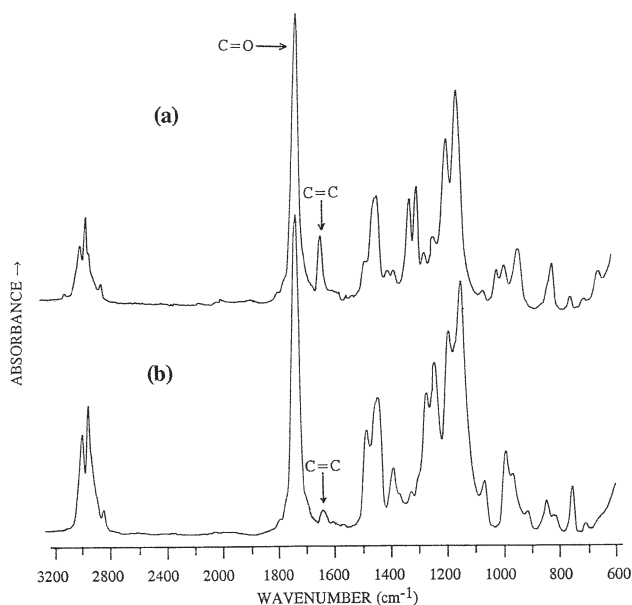


Figure 2 FTIR spectra of PMMA resin: (a) before reaction and (b) after reaction.

Basically, we determined the total quantity of peak of at 1630 cm^{-1} corresponding to the C=C double bonds available (D_A) of PMMA resin before reaction, and the residual amount of double bonds (D_B) in the reacted PMMA resin which underwent an isothermal reaction followed by a postcure at a heating rate of $10^\circ\text{C}/\text{min}$. In other words, the total degree of polymerization, P_{TOT} , determine from FTIR spectra was defined by

$$P_{\text{TOT}} = \frac{(D_A - D_B)}{D_A} \quad (1)$$

Table I given a summary of the values of P_{TOT} determined from FTIR spectra for the PMMA resin investigated.

Using DSC, we had determined the total heat generated Q_{TOT} , being the sum of the measured heat Q_T generated during an isothermal DSC run and the residual heat Q_R that was released when the sample was then heated to 150°C at the rate of $10^\circ\text{C}/\text{min}$, i.e.,

$$Q_{\text{TOT}} = Q_T + Q_R \quad (2)$$

To determine the conversion rate dP/dt and the conversion P (i.e., degree of reaction) during the isothermal reaction with the aid of thermograms (i.e., the rate of heat generated $(dQ/dt)_T$ obtained from isothermal DSC runs at temperature T), we had to estimate the ultimate heat Q_{UT} that would had been generated if complete conversion were achieved. This was because there are residual double bonds

remaining in the PMMA resin, as demonstrated above in Table I. Therefore, we have used the following expressions

$$\frac{dP}{dt} = \frac{1}{Q_{\text{UT}}} \left(\frac{dQ}{dt} \right)_T \quad (3)$$

and

$$P = \frac{1}{Q_{\text{UT}}} \int_{t_i}^t \left(\frac{dQ}{dt} \right)_T dt \quad (4)$$

where Q_{UT} is defined by

$$Q_{\text{UT}} = \frac{Q_{\text{TOT}}}{P_{\text{TOT}}} \quad (5)$$

Table I gives a summary of the values of P_{TOT} , Q_{TOT} , and Q_{UT} determined for the PMMA resins investigated. Using the data given in Table I and eqs. (3) and (4), we have analyzed the isothermal DSC runs, and the results were displayed in experimental data of Figures 3 and 4.

The mechanistic kinetic model used in this study to describe the reacted behavior of a PMMA resin was based on the following reaction. The rate equation was given by

$$\frac{dP}{dt} = -\eta k_{p0} (2[I]_o - [Z]_o) P^m \left(1 - \frac{P}{P_f} \right)^n \times (1 - \exp(-k_d(t - t_z))) \quad (6)$$

$$k_d = 6.879 \times 10^6 \exp\left(-\frac{7245.53}{T}\right) \quad (7)$$

$$k_{p0} = A_o \exp\left(-\frac{E_p}{RT}\right) \quad (8)$$

where dP/dt was the conversion rate, P was the conversion (i.e. degree of reaction), η was the initiator efficiency, k_{p0} was the rate constant of initial propagation, $[I]_o$ was the initial concentration of initiator, $[Z]_o$ was the initial concentration of retarder, P_f was the final conversion, m and n were the orders of reaction, k_d was the rate constant of initiation, t was the reaction time, t_z was the induction time before

TABLE I
Summary of the Heat Generated During Isothermal DSC Runs and Ultimate Degree of Polymerization of PMMA Resin

Summary	PMMA resin
Final degree of polymerization (P_{TOT}) ^a	0.725
Total heat of reaction (Q_{TOT}) (J/g)	258.4
Ultimate heat of reaction (Q_{UT}) (J/g)	356.4

^a At 90°C .

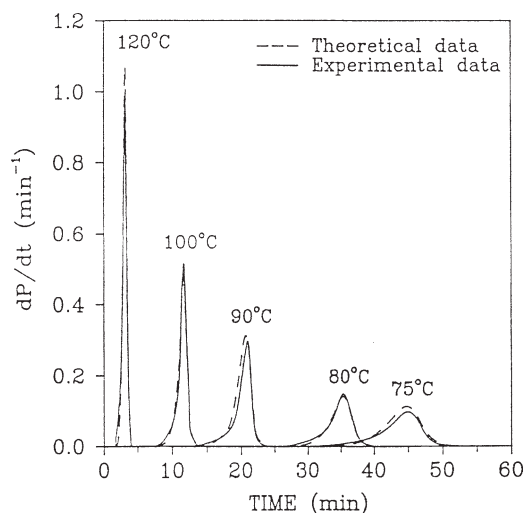


Figure 3 Comparison of experimental data (—) with theoretical predicted data (---) of conversion rate (dP/dt) versus reaction time for PMMA resin at various isothermal DSC runs.

propagation, A_0 was the preexponential factor of propagation, E_p was the activation energy of propagation, R was the universal gas constant.

Using initial conditions of $[Z]_0 = 6.936 \times 10^{-3}$ mol/L, $[I]_0 = 1.931 \times 10^{-2}$ mol/L, $P = 0$, and Figures 3 and 4 experimental data to solve eqs. (6) and (7) by a multiple regression technique, one can obtain that the kinetic parameters were described in Table II. From Table II, the average values was calculated as $m = 1.095$, $n = 0.893$. Using ηk_{po} data at 75–120°C to solve eq. (8) by linear regression method, it can be obtained that the kinetic parameters $\eta A_0 = 1.459 \times 10^9 \text{ min}^{-1}$, $E_p = 10.62 \text{ kcal/mol}$.

Figures 3 and 4 illustrate conversion rate (dP/dt) and conversion (P) versus time of PMMA resin form

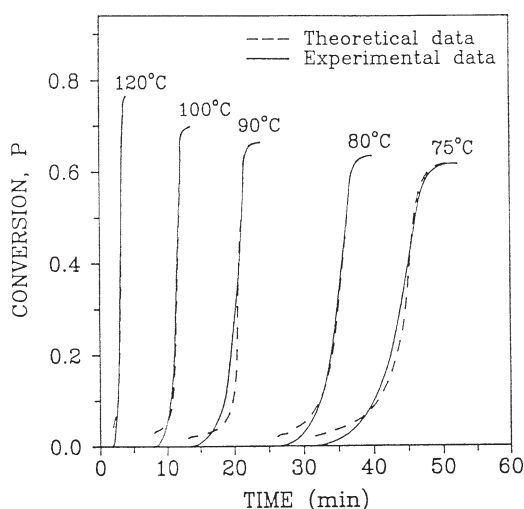


Figure 4 Comparison of experimental data (—) with theoretical predicted data (---) of conversion (P) versus reaction time for PMMA resin at various isothermal DSC runs.

the experimental and theoretical data at the isothermal runs. The dashed lines in Figures 3 and 4 represent the calculated values obtained from eq. (6) with the aforementioned kinetic parameters, and the solid lines were obtained directly from the DSC thermogram data by using eqs. (3)–(5). From Figures 3 and 4 results, one can observe that the experimental data agreed very well with the theoretical predictions.

Simulation results for a pultrusion process

The results obtained from the kinetic investigations were used to simulate the influence of system composition on temperature profiles inside the rectangular pultrusion die with size of $80 \times 1.25 \times 0.319 \text{ cm}$. To simplify the system, the following assumptions have been proposed: (1) the heat conduction is only in thickness direction; (2) the process is at steady state; (3) the diffusion of resin during reaction is negligible; (4) the velocity profile is flat; and (5) the local motion of resin during reaction is negligible.

From the above assumptions, the working equation of the model can be combined with kinetic expression and heat-transfer equations. They can be written as

$$-R_a = C_{ao} \frac{dP}{dt} = -C_{ao} \eta k_{po} (2[I]_0 - [Z]_0) \left(1 - \frac{P}{P_f}\right)^n P^m (1 - \exp(-k_d(t - t_z))) \quad (9)$$

$$\rho C_p v_z \frac{\partial T}{\partial z} = K_t \left(\frac{\partial^2 T}{\partial x^2}\right) + \Delta H \cdot R_a \quad (10)$$

where x was position in the thickness direction; C_{ao} was the initial concentration of the reactant (i.e., functional group in the resin) at the die entrance of $z = 0$; ρ was the bulk density; C_p was the bulk specific heat; K_t was the bulk thermal conductivity; R_a was the rate of formation of reacted resin; ΔH was the total heat; T was the temperature; v_z was the pulling speed; and z was in the axial (length) direction.

Note that the material being reacted consists of three components, namely, unreacted PMMA resin, glass fiber, and reacted PMMA resin. Therefore, the bulk physical properties of composite system were calculated from the following equation:

TABLE II
Summary of the Kinetic Parameters
Determined from Calculation

Temperature (°C)	ηk_{po} (min^{-1})	m	n
75	2.671×10^2	1.090	0.890
80	3.769×10^2	1.106	0.872
90	6.214×10^2	1.110	0.906
100	8.906×10^2	1.085	0.895
120	1.503×10^3	1.082	0.900

TABLE III
Physical Properties of the Materials Investigated

Materials	Density (g cm ⁻³)	Specific heat (cal/g-K)	Thermal conductivity (cal/cm-s-K)
Unreacted PMMA	1.04	-0.235 + 1.71 × 10 ⁻³ T	5.00 × 10 ⁻⁵
Reacted PMMA	1.15	-0.122 + 1.52 × 10 ⁻³ T	1.40 × 10 ⁻⁴
Glass fiber	2.54	0.197	2.08 × 10 ⁻³

$$\frac{1}{\rho} = \frac{W_m^o}{\rho_m} (1 - P) + \frac{W_m^o}{\rho_p} P + \frac{W_f}{\rho_f} \quad (11)$$

$$C_p = W_m C_{pm} + W_p C_{pp} + W_f C_{pf} \quad (12)$$

$$\frac{1}{K_t} = \frac{\phi_m}{K_{tm}} + \frac{\phi_p}{K_{tp}} + \frac{\phi_f}{K_{tf}} \quad (13)$$

where W was the weight fraction, ϕ was the volume fraction, and subscripts m^o , m , p , and f refer to resin, unreacted resin, reacted resin, and glass fiber, respectively. The boundary conditions for the model are given by

- (a) $x = x_o$ and $0 \leq z \leq L, T = T(z)$
(die wall temperature profile)
- (b) $z = 0$ and $0 \leq x \leq x_o, T = T_i$
(initial temperature of the system)
- (c) $x = 0$ and $0 \leq z \leq L, (\partial T / \partial x) = 0$
(symmetry condition)
- (14)

Equations (9) and (10) were solved in a numerically dimensionless way using a finite difference method. For numerical computation of the PMMA/glass fiber system, the experimentally determined values of the kinetic parameters were used that have been described in the previous sections. The physical properties of materials are given in Table III. The dimensions of the pultrusion die, the temperature of the material entering the die, and weight percent of glass fiber in the material were summarized in Table IV.

Figure 5 illustrates the temperature versus die position z (along the die length) for PMMA composites at various X values (die thickness direction/

half of die thickness). As shown in Figure 5, the dotted line represents the profile of the die wall temperature that was employed as the boundary [see eq. 14(a)] to solve eqs. (9) and (10).

From Figure 5, one can observe the following: (1) the thermal conductivity of both the resin and glass fiber (especially the resin) was very low (also seen in Table III) and the rate of heat transfer in the thickness direction (i.e., from the wall to the center of the die) was also very low; hence, a large temperature difference between the die wall and the center of the pultrusion die existed. (2) The reaction is exothermic, the temperature increasing further as the reaction continues. Consequently, the temperature at the center of the die (i.e., at $x = 0$) continues to increase even in the region where the die wall temperature was kept constant. (3) As the die wall temperature decreased near the end of the die, the temperature at the center of the die became higher than the die wall temperature. (4) From a comparison of curve b' (the experimental curve that was measured by using thermocouples imbedded in the die and curve b (the

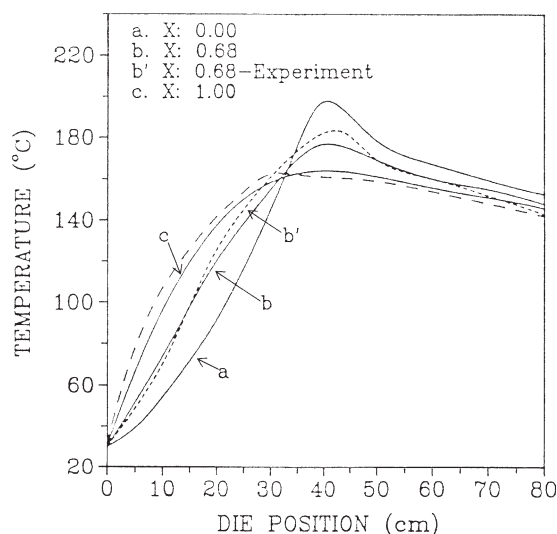


Figure 5 Temperature versus die position for PMMA composites at various values of X : (a) 0 (at center); (b) 0.68; (b') 0.68 (experiment); (c) 1.0 (at surface). The dotted curve is the temperature profile at the die wall imposed as boundary condition. The pulling speed, die thickness, and die temperature are 30 cm/min, 0.319 cm, and 140°C, respectively.

TABLE IV
Dimensions of Die and Feed Temperature
Used for Simulation

Materials	Die thickness (cm)	Die length (cm)	Feed temperature (°C)	Fiber content (wt %)
PMMA/GF	0.319	80	30	75

GF: glass fiber.

theoretical predicted from mathematical model), one can observe that the two curves agree very closely. This indicates that the mathematical model was in good agreement with the temperature profile predicted along the die length.

CONCLUSIONS

A mathematical model with a kinetic model and heat-transfer equation had been developed to predict the temperature profiles in a rectangular pultrusion die. The experimental results agreed very well with the theoretical prediction and indicated that the kinetic model $\frac{dP}{dt} = -\eta A_o \exp\left(-\frac{E_p}{RT}\right) (2[I]_o - [Z]_o)^m \left(1 - \frac{P}{P_f}\right)^n (1 - \exp(-k_d(t - t_z)))$ was suitable for glass fiber reinforced PMMA resin. The kinetic parameters $\eta A_o = 1.459 \times 10^9 \text{ min}^{-1}$, $E_p = 10.62 \text{ kcal/mol}$, $m = 1.095$, and $n = 0.893$ were obtained. It can be found that the theoretical predicted values of temperature profiles along the pultrusion die length were in good agreement with experimental data, which implied that the mathematical model was suitable for the pultrusion processes.

References

1. Suratno, B. R.; Ye, L.; Mai, Y. W. *Compos Sci Technol* 1998, 58, 191.
2. Joshi, S. C.; Lam, Y. C. *J Mater Proc Technol* 2006, 174, 178.
3. Luisier, A.; Bourban, P. E.; Manson, J. A. E. *Compos Part A: Appl Sci Manuf* 2003, 34, 583.
4. Yen, C. C.; Chen, C. H.; Lue, J. Y. *Polym Compos* 2006, 27, 8.
5. Chen, C. H.; Lien, K. C. *Polym Polym Compos* 2006, 14, 155.
6. Chen, C. H.; Chen, I. K. *Polym Compos* 2008, 29, 611.
7. Giordano, M.; Nicolais, L. *Polym Compos* 1997, 18, 681.
8. Britnell, D. J.; Tucker, N.; Smith, G. F.; Wong, S. S. F. *J Mater Proc Technol* 2003, 138, 311.
9. Zhu, J.; Chandrashekhara, K.; Flanigan, V.; Kapila, S. *Compos Part A: Appl Sci Manuf* 2004, 35, 95.
10. Baqkis, C. E.; Nanni, A.; Terosky, J. A.; Koehler, S. W. *Compos Sci Technol* 2001, 61, 815.
11. Turvey, G. J.; Zhang, Y. *Compos Part A: Appl Sci Manuf* 2005, 36, 309.
12. Boukhili, R.; Boukehili, H.; Daly, H. B.; Gasmi, A. *Polym Compos* 2006, 27, 71.
13. Boss, J. N.; Ganesh, V. K. *Compos Struct* 2006, 74, 289.
14. Li, J.; Joshi, S. C.; Lam, Y. C. *Compos Sci Technol* 2002, 62, 457.
15. Liu, X. L.; Crouch, I. G.; Lam, Y. C. *Compos Sci Technol* 2000, 60, 857.
16. Ding, Z.; Li, S.; Lee, L. J. *Polym Compos* 2002, 23, 957.
17. Lee, D. S.; Han, C. D. *J Appl Polym Sci* 1987, 34, 1235.
18. Astroom, B. T.; Pipes, R. B. *Polym Compos* 1993, 14, 184.
19. Han, C. D.; Chin, H. B. *Polym Eng Sci* 1988, 28, 321.
20. Liu, X. L.; Hillier, W. *Compos Struct* 1999, 47, 581.
21. Liu, X. L. *Compos Part A: Appl Sci Manuf* 2001, 32, 663.